Experiments and simulation models of a basic computation element of an autonomous molecular computing system

Masahiro Takinoue,[1,*] Daisuke Kiga,[2,†] Koh-ichiroh Shohda,[1,‡] and Akira Suyama[1,§]
[1]*Department of Life Sciences and Institute of Physics, The University of Tokyo, 3-8-1 Komaba, Meguro-ku, Tokyo 153-8902, Japan*
[2]*Department of Computational Intelligence and System Science, Tokyo Institute of Technology, 4259 Nagatsuta-cho, Midori-ku, Yokohama, Kanagawa 226-8503, Japan*
(Received 16 October 2007; revised manuscript received 20 June 2008; published 29 October 2008)

Autonomous DNA computers have been attracting much attention because of their ability to integrate into living cells. Autonomous DNA computers can process information through DNA molecules and their molecular reactions. We have already proposed an idea of an autonomous molecular computer with high computational ability, which is now named Reverse-transcription-and-TRanscription-based Autonomous Computing System (RTRACS). In this study, we first report an experimental demonstration of a basic computation element of RTRACS and a mathematical modeling method for RTRACS. We focus on an AND gate, which produces an output RNA molecule only when two input RNA molecules exist, because it is one of the most basic computation elements in RTRACS. Experimental results demonstrated that the basic computation element worked as designed. In addition, its behaviors were analyzed using a mathematical model describing the molecular reactions of the RTRACS computation elements. A comparison between experiments and simulations confirmed the validity of the mathematical modeling method. This study will accelerate construction of various kinds of computation elements and computational circuits of RTRACS, and thus advance the research on autonomous DNA computers.

DOI: 10.1103/PhysRevE.78.041921 PACS number(s): 87.15.A−, 89.20.Ff, 87.14.G−, 07.10.Cm

I. INTRODUCTION

A DNA computer is a bio-inspired computing machine that processes information through DNA molecules and their reactions. One of the attractive goals of DNA computer research is to realize a DNA computer able to integrate into living cells. Toward this goal, autonomous DNA computers have been intensively developed in recent years [1–8]. For instance, Shapiro *et al.* developed a DNA molecular automaton based on the class IIS restriction enzyme *Fok*I [1–3], and Hagiya *et al.* invented a state transition machine using a hairpin DNA molecule and a DNA polymerase (Whiplash PCR machine) [4–6]. The two computers exploit DNA molecules as programs and data, and use DNA molecules and enzymes as hardware. On the other hand, Seelig *et al.* developed enzyme-free nucleic acid logic circuits [7,8], which use DNA molecules as programs, data, and hardware. In its computing process, only DNA hybridization and branch migration reactions are used; no enzymes are used.

In our previous work, we proposed an autonomous molecular computer that has a higher computational ability than the above autonomous computers [9]. The computer is modeled after retroviral replication, and is now named Reverse-transcription-and-TRanscription-based Autonomous Computing System (RTRACS). In this system, DNA and RNA molecules are utilized as programs and data, respectively, and DNA and RNA molecules and enzymes are used as hardware. The computing process is autonomously carried out at a constant temperature with a reverse transcriptase, an RNA polymerase, a ribonuclease H, and a DNA polymerase. This computer has a distinguished feature: the computing system can be built up to meet demanding problems by combining modularized basic computation elements that can execute basic functions such as AND, OR, NOT, etc. The network of the basic computation elements connected by their input and output RNA molecules can form a computational circuit similar to integrated circuits in electronic computers. RTRACS is thus a splendid idea for constructing an autonomous molecular computer. However, no substantial experimental results on RTRACS have been reported.

In this study, we experimentally demonstrate one of the modularized basic computation elements of RTRACS. We also present a mathematical modeling method, which is essential for construction of various kinds of modularized basic computation elements. An AND gate of RTRACS was focused on because it is one of the most basic computation elements in RTRACS. The other computation elements can be constructed in the same manner as the AND gate. The behavior of the AND gate was experimentally examined, and the modeling method was validated by comparing the results of experiments and kinetic computer simulations. This study will advance autonomous DNA computers because it is the first report of experimental results and a mathematical modeling method of RTRACS with a high computational ability.

II. REACTION SCHEME OF THE AND GATE

In the AND gate of RTRACS, two RNA molecules are utilized as inputs, and one RNA molecule is created as an output after logical operation, which is achieved by a series of autonomously regulated hybridization and enzymatic reactions. The output RNA molecule is produced only when

*Present address: Department of Physics, Kyoto University, Kyoto 606-8502, Japan; takinoue@chem.scphys.kyoto-u.ac.jp
†kiga@dis.titech.ac.jp; http://www.sb.dis.titech.ac.jp/
‡shohda@genta.c.u-tokyo.ac.jp
§suyama@dna.c.u-tokyo.ac.jp; http://dna.c.u-tokyo.ac.jp/

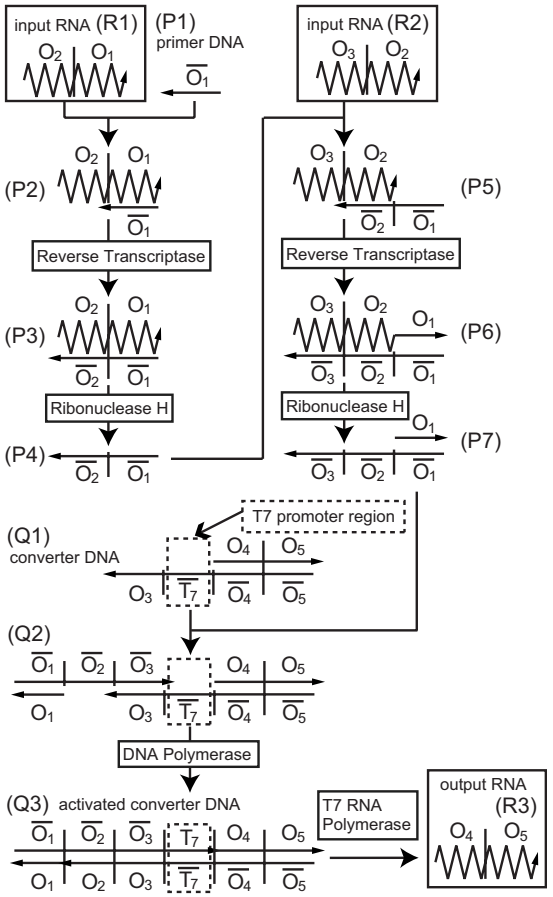

FIG. 1. Reaction scheme of the AND gate. An output RNA R3 is produced only when two input RNAs R1 and R2 exist. First, R1 hybridizes with a primer DNA P1 to form P2. P2 changes to P3 through DNA synthesis with reverse transcriptase; then P3 is turned into P4 by selective RNA degradation with ribonuclease H. P4 hybridizes with R2 to form P5. Likewise, P5 is turned into P7 with the enzymes. P7 hybridizes with a converter DNA Q1, and then they form Q2. Q2 is changed into an activated converter DNA Q3 through synthesis with DNA polymerase. Finally, T7 RNA polymerase transcribes R3 from Q3. The T7 RNA polymerase does not transcribe R3 from Q1 or Q2 with a single-stranded promoter because it can recognize only a double-stranded T7 promoter (T_7). RNA and DNA strands are represented by zigzag and linear arrows, respectively. They are composed of uniform-length orthonormal sequences from O_1 to O_5 and their complementary sequences from $\overline{O_1}$ to $\overline{O_5}$.

the two input RNA molecules are present. Figure 1 represents the reaction scheme of the AND gate. R1 and R2 are the input RNA molecules and R3 is the output RNA molecule. R3 is generated through intermediates, P1 to P7 and Q1 to Q3, only when both R1 and R2 exist.

At the beginning of the AND gate reaction, the input RNA R1 hybridizes with P1, a primer DNA, to form a DNA/RNA hybrid P2. R1 is a concatemer of sequences O_1 and O_2, and P1 has an $\overline{O_1}$ sequence that is complementary to O_1 and can hybridize with it. The zigzag arrows such as R1 and the linear arrows such as P1 indicate RNA and DNA strands, respectively.

The hybrid P2 is turned into P3 by extension with reverse transcriptase. Reverse transcriptase is an RNA-dependent DNA polymerase; this enzyme synthesizes a DNA strand complementary to an RNA template. Here, the reverse transcriptase synthesizes $\overline{O_2}$ using O_2 as a template. At the transition from P3 to P4, the RNA strand of the DNA/RNA hybrid P3 is degraded with ribonuclease H. The enzyme degrades the RNA strand of a DNA/RNA hybrid selectively. Here, the RNA strand O_2O_1 of P3 is degraded. The single-stranded DNA P4 hybridizes with the input RNA R2 to form a DNA/RNA hybrid P5. With reverse transcriptase, P5 changes to P6, and then P6 is turned into P7 with the ribonuclease H.

Subsequently, P7 hybridizes with Q1 (a converter DNA) to form Q2. Q2 is turned into Q3 (an activated converter DNA) by a DNA extension with DNA polymerase. This is a DNA-dependent DNA polymerase, which can synthesize a complementary DNA strand using its opposite strand as a template. Here, the DNA polymerase synthesizes complementary sequences to $\overline{T_7}$ and $\overline{O_2}$ in Q2. As a result, Q3 is created. In addition, the polymerase acts on P5 and synthesizes the DNA sequence O_1, so that P6 and P7 have a partly double-stranded DNA sequence (O_1-$\overline{O_1}$); however, this reaction is not essential for the AND gate.

At the end of the AND gate reaction, the output RNA R3 is transcribed from Q3 with T7 RNA polymerase, which is an enzyme that synthesizes an RNA strand using double-stranded DNA as a template. This reaction can start only when T7 RNA polymerase recognizes the double-stranded T7 promoter sequence, T_7. Here, the T7 RNA polymerase can recognize only Q3 but neither Q1 nor Q2 because Q1 and Q2 have single-stranded T_7. Thus, the output RNA R3 is produced only when both input RNAs R1 and R2 are present.

III. EXPERIMENTS ON THE AND GATE

A. Materials and methods

Nucleic acid sequences used in the AND gate reaction are shown in Fig. 2. To succeed in the AND gate reaction, it is important to design appropriate DNA/RNA sequences. Mishybridizations and undesired stable self-folded structures prevent correct AND gate reactions. The sequences of O_1 to O_5 were thus chosen from a set of orthonormal sequences developed for reliable DNA computing [10–12]. The orthonormal sequences have a uniform length, a uniform melting temperature, and have no potential for mishybridization or stable self-folded structures.

The orthonormal sequences O_1 to O_5 in R1, R2, R3, and Q1 were prefixed with *GGGAGA*, which is the sequence placed immediately after the T7 promoter region to increase the transcription activity. T7 RNA polymerase starts transcription at the first base *G* of the sequence *GGGAGA*. The prefixed orthonormal sequences were confirmed to remain orthonormal.

The reactions of the AND gate were performed by incubation for 30 min at 50 °C. The reaction buffer of the AND gate contained 40 m*M* Tris-HCl (*p*H 8.0), 50 m*M* NaCl, 13.8 m*M* $MgCl_2$, 2.0 m*M* Tris(2-carboxyethyl)phosphine (TCEP), 0.20 m*M* each dNTP, 2.0 m*M* ATP, 2.0 m*M* GTP,

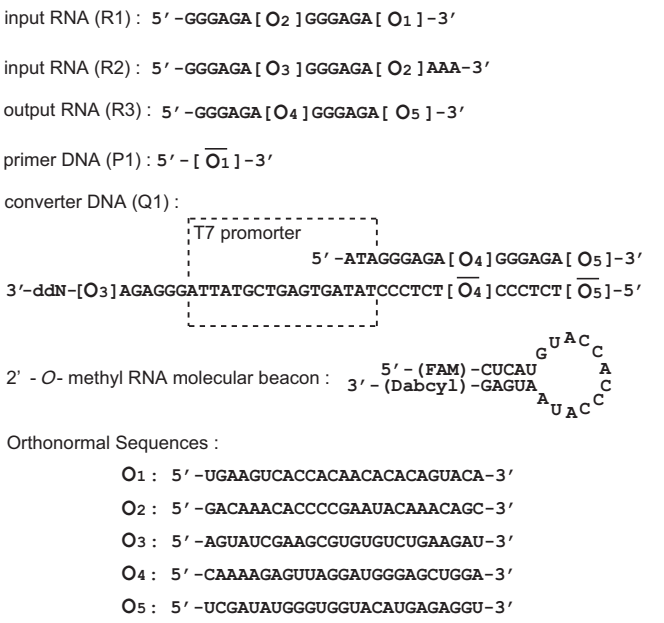

FIG. 2. Nucleic acid sequences used in experiments. All sequences were based on the orthonormal sequences O_1 to O_5, and three of their complementary sequences, $\overline{O_1}$, $\overline{O_4}$, and $\overline{O_5}$. R1, R2, and R3 are single-stranded RNA, and P1 is a single stranded DNA. Q1 partly forms a double helix, though most of the T7 promoter region remains single-stranded. The promoter region is enclosed by the broken-line box. The 3′ end of Q1 was modified by dideoxyribonucleoside (ddN) to avoid incorrect extension caused by mispriming. The 2′-O-methyl RNA molecular beacon with the fluorescent dye FAM, and the quencher Dabcyl, was designed to detect R3. It emits fluorescence only when hybridized with R3. The character *U*, used in O_1 to O_5 indicates the uracil base *U* for RNA strands R1, R2, and R3, but the thymine base *T* for DNA strands P1 and Q1.

2.0 m*M* CTP, 1.825 m*M* UTP, and 0.175 m*M* fluorescein-12-UTP. The initial concentrations of primer DNA, P1, and converter DNA, Q1, were 0.10 μM. The enzyme concentrations of avian myeloblastosis viruse (AMV) reverse transcriptase (Promega), Thermo T7 RNA polymerase (TOYOBO), and *Thermus thermophilus* ribonuclease H (TOYOBO) were 1.2 units/μl, 0.50 units/μl, and 50 μunits/μl, respectively. The AMV reverse transcriptase has three types of enzymatic activity: reverse transcriptase activity, DNA-dependent DNA polymerase activity, and ribonuclease H activity. Therefore, to simplify the system, no DNA polymerase was added, and the optimized concentration of *Thermus thermophilus* ribonuclease H was very low.

For the analysis of output RNA R3 by gel electrophoresis, the AND gate reaction was stopped with an equal volume of gel loading buffer (2×GLB) composed of 8.0 M urea, 10% (v/v) glycerol, 50 m*M* ethylenediaminetetraacetate (EDTA), and 0.05% (w/v) bromophenol blue (BPB). Then, 4.0 μl of the reaction solution was applied to a denaturing gel containing 8.0% polyacrylamide (acrylamide/bisacrylamide, 29:1) and 8.0 M urea. The running buffer for electrophoresis was Tris-borate-EDTA buffer (89 m*M* Tris-HCl, 89 m*M* boric acid, 2 m*M* EDTA, *p*H 8.3). The gel was run at constant voltage 250 V at constant temperature 65 °C. After electrophoresis, the output R3 in the gel was observed on a fluoroimage analyzer, FLA-5100 (Fuji Film), using fluorescence of the fluorescein-12-UTP included in R3 during the AND gate reaction. The reference R3 RNA marker was prepared by transcription from a completely double-stranded Q1 DNA in the presence of fluorescein-12-UTP.

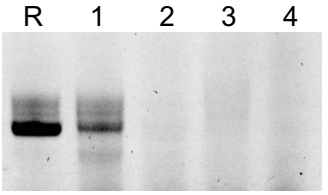

FIG. 3. Detection of output RNA R3 of AND gate reactions by gel electrophoresis. Lane 1: with two inputs ($[R1]_0=[R2]_0=0.10\ \mu M$). Lane 2: with only one input ($[R1]_0=0.10\ \mu M$, $[R2]_0=0\ \mu M$). Lane 3: with only one input ($[R1]_0=0\ \mu M$, $[R2]_0=0.10\ \mu M$). Lane 4: with no inputs ($[R1]_0=[R2]_0=0\ \mu M$). Lane R: a reference R3 RNA marker. $[R1]_0$ and $[R2]_0$ indicate the initial concentrations of inputs R1 and R2, respectively.

The kinetic analysis of the output R3 was carried out at 50 °C in the same buffer as was used for the gel electrophoresis analysis, except that 2.0 m*M* UTP and no fluorescein-12-UTP were used. The initial concentrations of P1 and Q1, and the enzyme concentrations of AMV reverse transcriptase, Thermo T7 RNA polymerase, and *Thermus thermophilus* ribonuclease H were the same as those used for the gel electrophoresis analysis. The reaction solutions of the kinetic experiments additionally contained 2.0 μM 2′-O-methyl RNA molecular beacon, which was designed to detect output RNA R3 (Fig. 2). The beacon emits fluorescence when it hybridizes with output RNA R3, while it does not emit fluorescence in the absence of the output RNA because of the fluorescence resonance energy transfer (FRET) between FAM and Dabcyl [13–15]. Using the molecular-beacon fluorescence, the R3 production was measured every 120 s on a real-time PCR apparatus, DNA Engine Opticon 2 (MJ Research, Inc.).

B. Results

First, we verified that the output R3 was produced only when the two input RNA molecules R1 and R2 were present, but it was not created in the other cases. Lane 1 in Fig. 3, which contained the reaction solution of the AND gate with two inputs R1 and R2, shows the presence of a transcriptional product, which had the same mobility as the reference R3 RNA marker in Lane R. The output R3 was thus correctly produced in the presence of the two inputs R1 and R2. In contrast, no transcriptional product was detected in Lanes 2, 3, and 4, which contained the reaction solution of the AND gate lacking either input R1 or input R2. Therefore, the reaction of the AND gate worked as designed Sec. II.

Next, we investigated input-output characteristics of the AND gate by observing its output production dependence on the initial concentrations of inputs (Fig. 4). When $[R2]_0$ was changed from 0 μM to 0.80 μM with $[R1]_0$ remaining at 0.10 μM, R3 production increased in proportion to $[R2]_0$ at

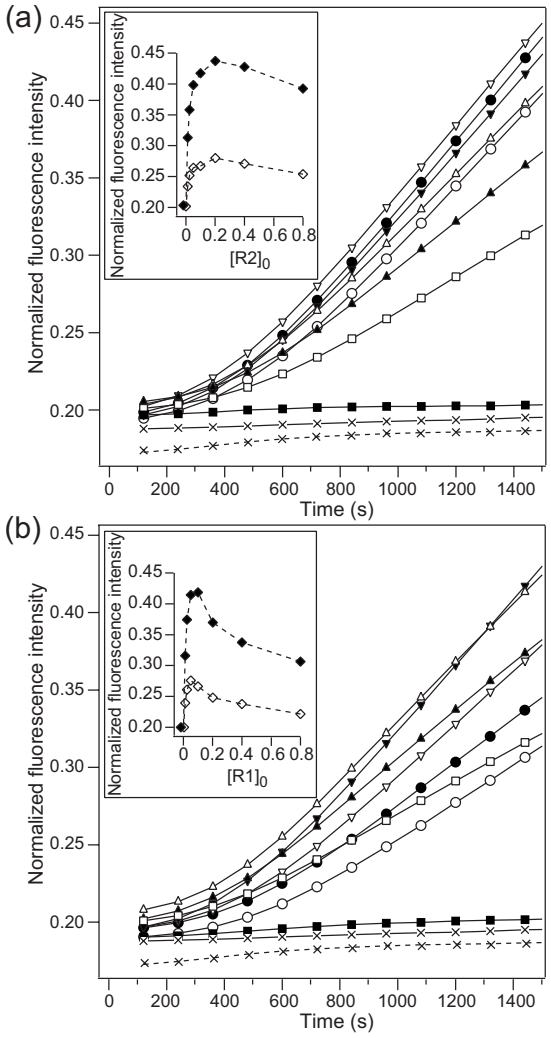

FIG. 4. Output production kinetics of AND gate in experiments. (a) $[R2]_0$ was changed from 0 μM to 0.80 μM with $[R1]_0$ remaining at 0.10 μM; $[R2]_0$=0.80 μM (open circle), 0.40 μM (filled circle), 0.20 μM (open inverted triangle), 0.10 μM (filled inverted triangle), 0.050 μM (open triangle), 0.025 μM (filled triangle), 0.0125 μM (open square), and 0 μM (filled square). The crosses with a solid line and a broken line indicate conditions of $[R1]_0$ $=[R2]_0=0$ μM with and without enzymes, respectively. Inset: dependence of R3 production on $[R2]_0$ at τ=720 s (open diamond) and 1440 s (filled diamond). (b) $[R1]_0$ was changed from 0 μM to 0.80 μM with $[R2]_0$ remaining at 0.10 μM; $[R1]_0$ =0.80 μM (open circle), 0.40 μM (filled circle), 0.20 μM (open inverted triangle), 0.10 μM (filled inverted triangle), 0.050 μM (open triangle), 0.025 μM (filled triangle), 0.0125 μM (open square), and 0 μM (filled square). The crosses with a solid or broken line indicate the same conditions as in (a). Inset: dependence of R3 production on $[R1]_0$ at τ=720 s (open diamond) and 1440 s (filled diamond). $[R1]_0$ and $[R2]_0$ are the initial concentrations of R1 and R2, respectively. The fluorescence intensity in these experiments was normalized by the fluorescence intensity at 95 °C.

$[R2]_0 \leqslant 0.20$ μM but decreased at $[R2]_0 > 0.20$ μM [Fig. 4(a)]. When $[R1]_0$ was changed from 0 μM to 0.80 μM with $[R2]_0$ remaining at 0.10 μM, R3 production increased in proportion to $[R1]_0$ at $[R1]_0 \leqslant 0.10$ μM but decreased at $[R1]_0 > 0.10$ μM [Fig. 4(b)]. The R3 production began to decrease at a lower initial concentration of $[R1]_0$ than that of $[R2]_0$. Therefore, $[R1]_0$ more strongly affected the decrease of R3 production than $[R2]_0$ did.

IV. NUMERICAL SIMULATIONS OF THE AND GATE

A. Simulation model

The first step of the AND gate reaction is a hybridization between R1 and P1. If the two-state model is assumed, the reaction is represented as

$$\mathrm{R1} + \mathrm{P1} \xrightarrow{k} \mathrm{P2}, \tag{1}$$

where k is the hybridization rate. The back reaction from P2 to R1+P1 need not be considered because the AND gate reaction was carried out under the condition that the double strand P2 is stable. Therefore, the rate equation for R1 is

$$\frac{d[\mathrm{R1}]}{dt} = -k[\mathrm{R1}][\mathrm{P1}]. \tag{2}$$

If the concentrations and time are normalized as

$$u_{\mathrm{R1}} \equiv \frac{[\mathrm{R1}]}{[\mathrm{Q1}]_0}, \quad u_{\mathrm{P1}} \equiv \frac{[\mathrm{P1}]}{[\mathrm{Q1}]_0},$$

$$\tau \equiv \frac{t}{(k[\mathrm{Q1}]_0)^{-1}}, \tag{3}$$

where $[Q1]_0$ is the initial concentration of Q1, the normalized rate equation is given as

$$\frac{du_{\mathrm{R1}}}{d\tau} = -u_{\mathrm{R1}}u_{\mathrm{P1}}. \tag{4}$$

The normalized rate equations for P1 and P2 in Eq. (1) are likewise

$$\frac{du_{\mathrm{P1}}}{d\tau} = -u_{\mathrm{R1}}u_{\mathrm{P1}}, \tag{5}$$

$$\frac{du_{\mathrm{P2}}}{d\tau} = u_{\mathrm{R1}}u_{\mathrm{P1}}. \tag{6}$$

The enzymatic reaction from P2 to P3 is represented using an assumption of the Michaelis-Menten model (see Appendix A 1) as follows:

$$\mathrm{E_{RT}} + \mathrm{P2} \underset{k_{-1}}{\overset{k_1}{\rightleftharpoons}} \mathrm{E_{RT}P2} \xrightarrow{k_2} \mathrm{E_{RT}} + \mathrm{P3}, \tag{7}$$

where E_{RT} indicates the reverse transcriptase, and k_1, k_{-1}, and k_2 represent the rate constants. The normalized rate equation is described as

$$\frac{du_{\mathrm{P2}}}{d\tau} = -\frac{du_{\mathrm{P3}}}{d\tau} = -\frac{1}{L_{\mathrm{P2}}}\frac{\nu_{\mathrm{RT}}u_{\mathrm{P2}}}{\kappa_{\mathrm{RT}} + u_{\mathrm{P2}}} = -\frac{u_{\mathrm{P2}}}{L_{\mathrm{P2}}}\frac{\nu_{\mathrm{RT}}}{\kappa_{\mathrm{RT}}}\left[1 + \frac{u_{\mathrm{P2}}}{\kappa_{\mathrm{RT}}}\right]^{-1}, \tag{8}$$

where ν_{RT} and κ_{RT} are normalized Michaelis-Menten parameters of reverse transcriptase. Since the Michaelis-Menten

parameters k_{catRT} and K_{mRT} for reverse transcriptase are represented as

$$k_{\mathrm{catRT}} \equiv k_2, \quad K_{\mathrm{mRT}} \equiv \frac{k_{-1}+k_2}{k_1}, \tag{9}$$

the normalized Michaelis-Menten parameters are defined as

$$\nu_{\mathrm{RT}} \equiv \frac{k_{\mathrm{catRT}}[\mathrm{E_{RT}}]_{\mathrm{T}}}{k[\mathrm{Q1}]_0^2}, \quad \kappa_{\mathrm{RT}} \equiv \frac{K_{\mathrm{mRT}}}{[\mathrm{Q1}]_0}, \tag{10}$$

where $[\mathrm{E_{RT}}]_{\mathrm{T}}$ is the total concentration of reverse transcriptase. The ν_{RT} is defined as the normalized extension rate per one base, so that Eq. (8) is divided by L_{P2}, the extension length for substrate P2.

The effect of a competition of substrates for reverse transcriptase should be included in the rate equation for the enzymatic reaction from P2 to P3. Reverse transcriptase generally has ribonuclease H activity and DNA polymerase activity as well as reverse transcriptase activity [16]. Therefore, the reverse transcriptase competitively acts on the substrates P2 and P5 through reverse transcriptase activity, P3 and P6 through ribonuclease H activity, and Q2 through DNA polymerase activity. This creates a competition of the substrates for the enzyme. The competitive enzymatic reactions are represented as

$$\begin{aligned} &\overset{\mathrm{RT}}{\mathrm{P2}\rightarrow\mathrm{P3}},\\ &\overset{\mathrm{RT}}{\mathrm{P5}\rightarrow\mathrm{P6}},\\ &\overset{\mathrm{RH}'}{\mathrm{P3}\rightarrow\mathrm{P4}},\\ &\overset{\mathrm{RH}'}{\mathrm{P6}\rightarrow\mathrm{P7}},\\ &\overset{\mathrm{DP}'}{\mathrm{Q2}\rightarrow\mathrm{Q3}}, \end{aligned} \tag{11}$$

where RT, RH′, and DP′ are the reverse transcriptase activity, ribonuclease H activity, and DNA polymerase activity of the reverse transcriptase, respectively. Because of the competition reactions for the reverse transcriptase, the enzymatic rate equation, Eq. (8), must be changed to

$$\frac{du_{\mathrm{P2}}}{d\tau} = -\frac{du_{\mathrm{P3}}}{d\tau} = -\frac{u_{\mathrm{P2}}}{L_{\mathrm{P2}}}\beta_{\mathrm{RT}}, \tag{12}$$

where

$$\beta_{\mathrm{RT}} = \frac{\nu_{\mathrm{RT}}}{\kappa_{\mathrm{RT}}}\left[1+\frac{u_{\mathrm{P2}}}{\kappa_{\mathrm{RT}}}+\frac{u_{\mathrm{P5}}}{\kappa_{\mathrm{RT}}}+\frac{u_{\mathrm{P3}}}{\kappa_{\mathrm{RH}'}}+\frac{u_{\mathrm{P6}}}{\kappa_{\mathrm{RH}'}}+\frac{u_{\mathrm{Q2}}}{\kappa_{\mathrm{DP}'}}\right]^{-1}. \tag{13}$$

$\kappa_{\mathrm{RH}'}$ and $\kappa_{\mathrm{DP}'}$ are normalized Michaelis-Menten parameters for the ribonuclease H activity and DNA polymerase activity of reverse transcriptase. The parameters are defined as in Eq. (10). The term $u_{\mathrm{P2}}/\kappa_{\mathrm{RT}}$ in Eq. (13) is the contribution from reverse transcriptase activity, which is the same as the term $u_{\mathrm{P2}}/\kappa_{\mathrm{RT}}$ in Eq. (8). The term $u_{\mathrm{P5}}/\kappa_{\mathrm{RT}}$ is also a contribution from reverse transcriptase activity, which is added to the equation because of the competition. The terms $u_{\mathrm{P3}}/\kappa_{\mathrm{RH}'}$ and $u_{\mathrm{P6}}/\kappa_{\mathrm{RH}'}$ are contributions from ribonuclease H activity, and the term $u_{\mathrm{Q2}}/\kappa_{\mathrm{DP}'}$ is the contribution from DNA polymerase activity. These are additional contributions caused by the competitive enzymatic reactions. The derivation of this rate equation is explained in Appendix A 2.

Finally, the rate equation for P2 is obtained by summing the hybridization step from R1+P1 to P2 and the reverse transcription step from P2 to P3 as follows:

$$\frac{du_{\mathrm{P2}}}{d\tau} = u_{\mathrm{R1}}u_{\mathrm{P1}} - \frac{\beta_{\mathrm{RT}}u_{\mathrm{P2}}}{L_{\mathrm{P2}}}, \tag{14}$$

where the first term indicates the hybridization in Eq. (6), and the second term represents the reverse transcription in Eq. (12).

The rate equation for P3 can be obtained similarly by considering the competitive enzymatic reactions. The step from P3 to P4 proceeds using ribonuclease H activity. This activity is competitively provided by both ribonuclease H and reverse transcriptase. This case represents the competition of enzymes for the substrate. Competition of substrates for the enzyme should also be included. The reverse transcriptase competitively acts on the substrates P2, P5, P3, P6, and Q2, as already explained, and the ribonuclease H competitively acts on P3 and P6. Thus, competitive reactions can be summarized as follows:

$$\begin{aligned} &\overset{\mathrm{RT}}{\mathrm{P2}\rightarrow\mathrm{P3}},\\ &\overset{\mathrm{RT}}{\mathrm{P5}\rightarrow\mathrm{P6}},\\ &\overset{\mathrm{RH}'/\mathrm{RH}}{\mathrm{P3}\rightarrow\mathrm{P4}},\\ &\overset{\mathrm{RH}'/\mathrm{RH}}{\mathrm{P6}\rightarrow\mathrm{P7}},\\ &\overset{\mathrm{DP}'}{\mathrm{Q2}\rightarrow\mathrm{Q3}}, \end{aligned} \tag{15}$$

where RT, RH′, and DP′ are the reverse transcriptase activity, ribonuclease H activity, and DNA polymerase activity of the reverse transcriptase, respectively, and RH is the ribonuclease H activity of ribonuclease H. Therefore, the rate equation of the step from P3 to P4 is described as

$$\frac{du_{\mathrm{P3}}}{d\tau} = -\frac{du_{\mathrm{P4}}}{d\tau} = -\beta_{\mathrm{RH}}u_{\mathrm{P3}}, \tag{16}$$

where it is assumed that the RNA degradation rate by ribonuclease H activity, β_{RH}, is a value per one DNA/RNA hybrid not per one base, because ribonuclease H activity cleaves the RNA strand only at some internal phosphate bonds of the strand and does not break the strand into mononucleotides. Therefore, the right-hand side of Eq. (16) is not divided by the DNA/RNA hybrid length in contrast to Eq. (12). The value β_{RH} is represented as follows:

$$\beta_{\mathrm{RH}} = \frac{\nu_{\mathrm{RH}}}{\kappa_{\mathrm{RH}}}\left[1 + \frac{u_{\mathrm{P3}}}{\kappa_{\mathrm{RH}}} + \frac{u_{\mathrm{P6}}}{\kappa_{\mathrm{RH}}}\right]^{-1} + \frac{\nu_{\mathrm{RH}'}}{\kappa_{\mathrm{RH}'}}\left[1 + \frac{u_{\mathrm{P2}}}{\kappa_{\mathrm{RT}}} + \frac{u_{\mathrm{P5}}}{\kappa_{\mathrm{RT}}} + \frac{u_{\mathrm{P3}}}{\kappa_{\mathrm{RH}'}} + \frac{u_{\mathrm{P6}}}{\kappa_{\mathrm{RH}'}} + \frac{u_{\mathrm{Q2}}}{\kappa_{\mathrm{DP}'}}\right]^{-1}, \tag{17}$$

where ν_{RH} and κ_{RH}, which are defined as in Eq. (10), are normalized Michaelis-Menten parameters for the ribonuclease H activity of ribonuclease H. Likewise, $\nu_{\mathrm{RH}'}$ and $\kappa_{\mathrm{RH}'}$ are normalized Michaelis-Menten parameters for the ribonuclease H activity of reverse transcriptase. The first term of the right-hand side of Eq. (17) is the contribution from ribonuclease H, and the second term is the contribution from reverse transcriptase (see Appendixes A 2 and A 3). By the reverse transcription from P2 to P3 in Eq. (12) and the RNA degradation from P3 to P4 in Eq. (16), the rate equation for P3 is obtained as

$$\frac{du_{\mathrm{P3}}}{d\tau} = \frac{\beta_{\mathrm{RT}} u_{\mathrm{P2}}}{L_{\mathrm{P2}}} - \beta_{\mathrm{RH}} u_{\mathrm{P3}}. \tag{18}$$

The rate equations for P4, P5, P6, and P7 can be derived likewise. In the step from P4 to P5, hybridization between P4 and R2 makes the duplex P5. By combining this hybridization with the RNA degradation from P3 to P4 in Eq. (16), the rate equation for P4 becomes

$$\frac{du_{\mathrm{P4}}}{d\tau} = \beta_{\mathrm{RH}} u_{\mathrm{P3}} - u_{\mathrm{R2}} u_{\mathrm{P4}}. \tag{19}$$

The hybridization rate between P4 and R2 was assumed to be the same as the one between P1 and R1 because the two hybrids P4-R2 and P1-R1 have a duplex region (O_2-$\overline{O_2}$ and O_1-$\overline{O_1}$, respectively) of the same length. The rate equation for R2 is thus represented as

$$\frac{du_{\mathrm{R2}}}{d\tau} = - u_{\mathrm{R2}} u_{\mathrm{P4}}. \tag{20}$$

The step from P5 to P6 is a reverse transcription just like the step from P2 to P3, which is the competitive enzymatic reaction of reverse transcriptase in Eq. (11). This step is represented as

$$\frac{du_{\mathrm{P5}}}{d\tau} = - \frac{du_{\mathrm{P6}}}{d\tau} = - \frac{\beta_{\mathrm{RT}} u_{\mathrm{P5}}}{L_{\mathrm{P5}}}. \tag{21}$$

Therefore, the rate equation for P5 can be described by considering Eq. (21) and the hybridization between P4 and R2 as follows:

$$\frac{du_{\mathrm{P5}}}{d\tau} = u_{\mathrm{R2}} u_{\mathrm{P4}} - \frac{\beta_{\mathrm{RT}} u_{\mathrm{P5}}}{L_{\mathrm{P5}}}. \tag{22}$$

The step from P6 to P7 is an RNA degradation by ribonuclease H activity just like the step from P3 to P4. It is a competitive reaction of ribonuclease H and reverse transcriptase in Eq. (15). The rate equation of P6 to P7 is thus described as

$$\frac{du_{\mathrm{P6}}}{d\tau} = - \frac{du_{\mathrm{P7}}}{d\tau} = \frac{\beta_{\mathrm{RT}} u_{\mathrm{P5}}}{L_{\mathrm{P5}}}. \tag{23}$$

By considering this RNA degradation and the reverse transcription from P5 to P6, the rate equation for P6 is obtained as

$$\frac{du_{\mathrm{P6}}}{d\tau} = \frac{\beta_{\mathrm{RT}} u_{\mathrm{P5}}}{L_{\mathrm{P5}}} - \beta_{\mathrm{RH}} u_{\mathrm{P6}}. \tag{24}$$

P7, which is created at the RNA degradation step from P6 to P7, hybridizes with Q1 to form Q2. Therefore, the rate equation for P7 becomes

$$\frac{du_{\mathrm{P7}}}{d\tau} = \beta_{\mathrm{RH}} u_{\mathrm{P6}} - u_{\mathrm{P7}} u_{\mathrm{Q1}}. \tag{25}$$

The rate equations for Q1, Q2, and Q3 can be derived from the rate equations for hybridization and DNA polymerization. The rate equation for Q1 includes only the hybridization with P7 and is represented as

$$\frac{du_{\mathrm{Q1}}}{d\tau} = - u_{\mathrm{P7}} u_{\mathrm{Q1}}, \tag{26}$$

where the hybridization rate was assumed to be k because the length of a duplex region in the hybrid is the same as that in the P1-R1 hybrid. The rate equation for Q2 includes the hybridization of P7 with Q1 and DNA polymerization from Q2 to Q3. The step from Q2 to Q3 is supported by DNA polymerase and reverse transcriptase. The two enzymes competitively react on the substrate Q2 to produce Q3. This case represents a competition of enzymes for a substrate. Competition of substrates for an enzyme also takes place; the reverse transcriptase competitively acts on the substrates P2, P5, P3, P6, and Q2. Thus, competitive reactions about the DNA polymerase activity of the two enzymes are represented as

$$\begin{aligned} &\mathrm{P2} \xrightarrow{\mathrm{RT}} \mathrm{P3}, \\ &\mathrm{P3} \xrightarrow{\mathrm{RH}'} \mathrm{P4}, \\ &\mathrm{P5} \xrightarrow{\mathrm{RT}} \mathrm{P6}, \\ &\mathrm{P6} \xrightarrow{\mathrm{RH}'} \mathrm{P7}, \\ &\mathrm{Q2} \xrightarrow{\mathrm{DP}'/\mathrm{DP}} \mathrm{Q3}, \end{aligned} \tag{27}$$

where RT, RH′, and DP′ are the reverse transcriptase activity, ribonuclease H activity, and DNA polymerase activity of the reverse transcriptase, respectively. DP is the DNA polymerase activity of DNA polymerase. Therefore, the rate equation for the DNA polymerization from Q2 to Q3 is derived as

$$\frac{du_{Q3}}{d\tau} = -\frac{du_{Q2}}{d\tau} = \frac{\beta_{DP} u_{Q2}}{L_{Q2}}, \tag{28}$$

where L_{Q2} is the DNA extension length and

$$\beta_{DP} = \frac{\nu_{DP}}{\kappa_{DP}}\left[1 + \frac{u_{Q2}}{\kappa_{DP}}\right]^{-1} + \frac{\nu_{DP'}}{\kappa_{DP'}}\left[1 + \frac{u_{P2}}{\kappa_{RT}} + \frac{u_{P5}}{\kappa_{RT}} + \frac{u_{P3}}{\kappa_{RH'}} + \frac{u_{P6}}{\kappa_{RH'}} + \frac{u_{Q2}}{\kappa_{DP'}}\right]^{-1}. \tag{29}$$

ν_{DP} and κ_{DP} are normalized Michaelis-Menten parameters of the DNA polymerase activity of DNA polymerase, and $\nu_{DP'}$ and $\kappa_{DP'}$ are those of reverse transcriptase. The first term of the right-hand side of Eq. (29) represents the contribution from DNA polymerase, and the second term is the contribution from reverse transcriptase. The derivation of this equation is explained in Appendixes A 2 and A 3. As a result of the competition, Eq. (28), and the hybridization of P7 and Q1, the rate equations for Q2 are

$$\frac{du_{Q2}}{d\tau} = u_{P7} u_{Q1} - \frac{\beta_{DP} u_{Q2}}{L_{Q2}}, \tag{30}$$

where the first term indicates the hybridization between P7 and Q1, and the second term is the DNA polymerization. Q3 is only produced by the DNA polymerization step, and the rate equation for Q3 is represented as

$$\frac{du_{Q3}}{d\tau} = \frac{\beta_{DP} u_{Q2}}{L_{Q2}}. \tag{31}$$

The rate equation for output R3, which is transcribed using Q3 as a substrate, is represented as

$$\frac{du_{R3}}{d\tau} = \frac{\beta_{RP} u_{Q3}}{L_{Q3}}, \tag{32}$$

where L_{Q3} is the length of R3 and

$$\beta_{RP} = \frac{\nu_{RP}}{\kappa_{RP}}\left[1 + \frac{u_{Q3}}{\kappa_{RP}}\right]^{-1}. \tag{33}$$

ν_{RP} and κ_{RP} are normalized Michaelis-Menten parameters for the RNA polymerase activity of RNA polymerase.

Finally, a set of equations used to describe the AND gate reaction is as follows: Eqs. (4), (5), (14), (18)–(20), (22), (24)–(26), and (30)–(32), which represent the rate equations, and Eqs. (13), (17), (29), and (33), which represent the rate coefficients of the enzymatic reactions.

B. Back-hybridization

In addition to the reactions shown in Fig. 1, the AND gate includes some inhibitory reactions that delay output RNA production. The inhibitory reactions are shown in Fig. 5 as the broken lines BH1, BH2, and BH3. BH1 is the back-hybridization of P4 with R1. P4 hybridizes with R2; however, P4 can also hybridize with R1 because P4 has a perfectly complementary sequence to R1. BH2 is the back-hybridization of P7 with R2. Although P7 hybridizes with Q1, it can also hybridize with R2 in a similar way. BH3 is the back-hybridization of P7 with R1. P7 has a partly complementary sequence to R1. P7 and R1 thus hybridize with each other and form P8. BH3 does not delay the AND gate reactions more than the back-hybridizations BH1 and BH2, because P8 can hybridize with Q1 as P7 can (broken line BH3″). BH3 only limits output production due to its wasteful spending of input RNA, R1.

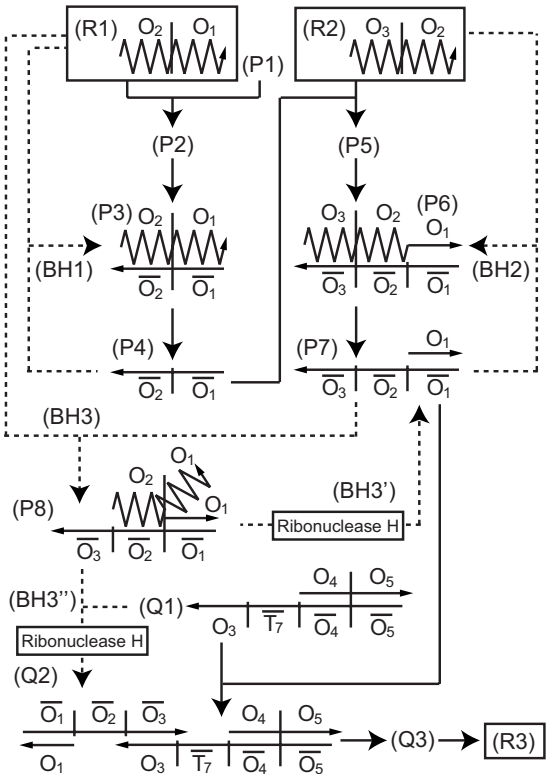

FIG. 5. AND gate reaction scheme including back-hybridizations. Only molecules involved in back-hybridizations are illustrated; the others are represented by their molecular names. The back-hybridizations are represented by broken lines, BH1, BH2, and BH3. BH1 is the back-hybridization of P4 with R1; BH2 is the back-hybridization of P7 with R2; and BH3 is the back-hybridization of P7 with R1. The molecule P8 is a new complex created by BH3. The broken lines BH3′ and BH3″ are reactions incidental to BH3. BH3′ is an RNA degradation with ribonuclease H, and BH3″ is a hybridization of P8 with Q1.

Due to the back-hybridizations, Eqs. (4), (18)–(20), (24)–(26), and (30) are partly modified. The modified rate equations are described as

$$(4) \Rightarrow \frac{du_{R1}}{d\tau} = -u_{R1}u_{P1} + \{-2u_{R1}u_{P4} - u_{R1}u_{P7}\}, \tag{34}$$

$$(18) \Rightarrow \frac{du_{P3}}{d\tau} = \frac{\beta_{RT}u_{P2}}{L_{P2}} - \beta_{RH}u_{P3} + \{2u_{R1}u_{P4}\}, \tag{35}$$

$$(19) \Rightarrow \frac{du_{P4}}{d\tau} = \beta_{RH}u_{P3} - u_{R2}u_{P4} + \{-2u_{R1}u_{P4}\}, \tag{36}$$

$$(20) \Rightarrow \frac{du_{R2}}{d\tau} = -u_{R2}u_{P4} + \{-2u_{R2}u_{P7}\}, \tag{37}$$

$$(24) \Rightarrow \frac{du_{P6}}{d\tau} = \frac{\beta_{RT}u_{P5}}{L_{P5}} - \beta_{RH}u_{P6} + \{2u_{R2}u_{P7}\}, \tag{38}$$

$$(25) \Rightarrow \frac{du_{P7}}{d\tau} = \beta_{RH}u_{P6} - u_{P7}u_{Q1} + \{\beta_{RH}u_{P8} - u_{R1}u_{P7} - 2u_{R2}u_{P7}\}, \tag{39}$$

$$(26) \Rightarrow \frac{du_{Q1}}{d\tau} = -u_{P7}u_{Q1} + \{-u_{P8}u_{Q1}\}, \tag{40}$$

$$(30) \Rightarrow \frac{du_{Q2}}{d\tau} = u_{P7}u_{Q1} - \frac{\beta_{DP}u_{Q2}}{L_{Q2}} + \{u_{P8}u_{Q1}\}, \tag{41}$$

where the terms added by the back-hybridizations are enclosed in braces to emphasize the modifications. In addition, the following rate equation must be added to describe P8, which is a new species created by the back-hybridization BH3:

$$\frac{du_{P8}}{d\tau} = +\{u_{R1}u_{P7} - u_{P8}u_{Q1} - \beta_{RH}u_{P8}\}. \tag{42}$$

Polynucleotide hybridization rates depend on the square root of the strand length because nucleation sites become less available as the strand length increases due to excluded volume effect [17]. We assumed that the hybridization rate was in proportion to the hybridization site length because the site length was short compared to polynucleotide strands. It was also assumed that the hybridization rate did not depend on the base sequence of the hybridization site because the site had an orthonormal sequence. The hybridization rate of the back-hybridization BH3 was thus set to be k, which is the same value as the hybridization rate of P1 and R1 with the same hybridization site length. On the other hand, the hybridization rates of the back-hybridizations BH1 and BH2 were set to be $2k$, because BH1 and BH2 have a hybridization site of a double length.

The rate coefficients of enzymatic activities, β_{RT}, β_{RH}, β_{DP}, are also changed because of the back-hybridizations. Equations (13), (17), and (29) are modified as follows:

$$(13) \Rightarrow \beta_{RT} = \frac{\nu_{RT}}{\kappa_{RT}}\left[1 + \frac{u_{P2}}{\kappa_{RT}} + \frac{u_{P5}}{\kappa_{RT}} + \frac{u_{Q2}}{\kappa_{DP'}} + \frac{u_{P3}}{\kappa_{RH'}} + \frac{u_{P6}}{\kappa_{RH'}} + \left\{\frac{u_{P8}}{\kappa_{RH'}}\right\}\right]^{-1}, \tag{43}$$

$$(17) \Rightarrow \beta_{RH} = \frac{\nu_{RH}}{\kappa_{RH}}\left[1 + \frac{u_{P3}}{\kappa_{RH}} + \frac{u_{P6}}{\kappa_{RH}} + \left\{\frac{u_{P8}}{\kappa_{RH}}\right\}\right]^{-1} + \frac{\nu_{RH'}}{\kappa_{RH'}}\left[1 + \frac{u_{P2}}{\kappa_{RT}} + \frac{u_{P5}}{\kappa_{RT}} + \frac{u_{Q2}}{\kappa_{DP'}} + \frac{u_{P3}}{\kappa_{RH'}} + \frac{u_{P6}}{\kappa_{RH'}} + \left\{\frac{u_{P8}}{\kappa_{RH'}}\right\}\right]^{-1}. \tag{44}$$

$$(29) \Rightarrow \beta_{DP} = \frac{\nu_{DP}}{\kappa_{DP}}\left[1 + \frac{u_{Q2}}{\kappa_{DP}}\right]^{-1} + \frac{\nu_{DP'}}{\kappa_{DP'}}\left[1 + \frac{u_{P2}}{\kappa_{RT}} + \frac{u_{P5}}{\kappa_{RT}} + \frac{u_{Q2}}{\kappa_{DP'}} + \frac{u_{P3}}{\kappa_{RH'}} + \frac{u_{P6}}{\kappa_{RH'}} + \left\{\frac{u_{P8}}{\kappa_{RH'}}\right\}\right]^{-1}, \tag{45}$$

where $u_{P8}/\kappa_{RH'}$ is the contribution from the RNA degradation represented by the broken line BH3′.

Finally, considering the back-hybridizations, a set of equations used to describe the AND gate reaction is as follows: Eqs. (5), (14), (22), (31), (32), and (34)–(42), which represent the rate equations, and Eqs. (33) and (43)–(45), which represent the rate coefficients of enzymatic reactions.

C. Model parameters

Kinetic simulations for the rate equations of the AND gate were carried out using the fourth-order Runge-Kutta method. In the simulations, we used the Michaelis-Menten parameters reported in other biochemical research: AMV reverse transcriptase ($K_{mRT}=K_{mDP'}=K_{mRH'}=0.01\ \mu M$, $k_{catRT}=2\ s^{-1}$, $k_{catDP'}=k_{catRT}/3$, $k_{catRH'}=k_{catRT}/1200$) [18,19], T7 RNA polymerase ($K_{mRP}=0.026\ \mu M$, $k_{catRP}=0.9\ s^{-1}$) [20], and *Thermus thermophilus* ribonuclease H ($K_{mRH}=0.13\ \mu M$, $k_{catRH}=0.082\ s^{-1}$) [21]. As the K_m value per base pair of the *Thermus thermophilus* ribonuclease H was reported as $7.8\ \mu M$ [21], K_{mRH} (the K_m value per DNA-RNA hybrid) was set at $0.13\ \mu M$ by assuming that DNA-RNA hybrids included 62 base pairs. The values of L_{P2}, L_{P5}, L_{Q2}, and L_{Q3} were assumed to be 37, 31, 14, and 62, respectively, and were the nucleic acid lengths used in the experiments. The hybridization rate k was set at $10\ \mu M^{-1}\ s^{-1}$, based on our measurements from experiments using the same buffer and temperature conditions.

Enzyme concentrations in the simulations were the same as in the experiments. In the experimental section III A, the total enzyme concentrations were represented as the unit definition of enzymes. Their values were thus converted to molar concentrations for numerical simulations: $[E_{RT}]_T=1.0\ \mu M$ (AMV reverse transcriptase), $[E_{RP}]_T=0.15\ \mu M$ (Thermo T7 RNA polymerase), $[E_{RH}]_T=1.7\times10^{-5}\ \mu M$ (*Thermus thermophilus* ribonuclease H), and $[E_{DP}]_T=0\ \mu M$ (DNA polymerase). These values were calculated using enzyme data sheets distributed by the enzyme manufacturers and the above Michaelis-Menten parameters.

Nucleic acid concentrations were also the same as in the experiments. $u_{P1}(0)$ and $u_{Q1}(0)$ were set at 1, where $u_{P1}(0)$ and $u_{Q1}(0)$ are the normalized initial concentrations of P1 and Q1. $u_{R1}(0)$ and $u_{R2}(0)$ were changed from 0 to 8, where $u_{R1}(0)$ and $u_{R2}(0)$ are the normalized initial concentrations of input RNA R1 and R2. The value 1 for a normalized concentration represents $0.1\ \mu M$ in the experiment because all the normalized concentrations were normalized by the initial concentration of Q1, $[Q1]_0$ ($=0.10\ \mu M$).

D. Results

The output dependence of the AND gate on the initial concentrations of inputs was analyzed by kinetic simulations for

the rate equations of the AND gate. The simulations were carried out using the models with and without back-hybridizations. In the simulations without back-hybridizations, the production of output RNA R3 monotonically increased with the initial concentrations of input RNA R1 and R2 (data not shown). On the other hand, in the simulations with back-hybridizations, the production of output R3 increased at lower initial concentrations of inputs but slightly decreased at higher initial concentrations of inputs (Fig. 6). When the normalized concentration $u_{R2}(0)$ of input R2 was changed from 0.125 to 8 with the normalized concentration $u_{R1}(0)$ of input R1 remaining at 1, R3 production increased in the case of $u_{R2}(0)<2$ and slightly decreased in the case of $u_{R2}(0)>2$ [Fig. 6(a)]. When $u_{R1}(0)$ was changed from 0.125 to 8 with $u_{R2}(0)$ remaining at 1, R3 production increased in the case of $u_{R1}(0)<1$ and slightly decreased in the case of $u_{R1}(0)>1$ [Fig. 6(b)]. R3 production began to decrease at a lower input concentration when $u_{R1}(0)$ was changed than when $u_{R2}(0)$ was changed. Therefore, R1 more strongly affected the decrease of R3 production than R2 did.

The results of the kinetic simulations were compared with those of the experiments in Fig. 4. For the comparison, it is necessary to know the relationship between the scales of the axes. In the case of the time axis, $\tau=1500$ in the simulations corresponds to 1500 s in the experiments because of $k=10\ \mu M^{-1}\ s^{-1}$, $[Q1]_0=0.10\ \mu M$ and Eq. (3). In the case of the output production axis, the normalized concentration of the output R3 in the simulations is proportional to the normalized fluorescence intensity from R3 in the experiments because the fluorescence intensity increased with the actual concentration of R3.

As a result of the comparison between the simulations and the experiments, the simulations with back-hybridizations explained well the results of the experiments. The results of both the simulations with back-hybridizations and the experiments demonstrated that R3 production increased at lower initial concentrations of inputs R1 and R2, but it decreased at higher initial input concentrations. Moreover, in both sets of results, the initial concentrations of the input R1 more strongly affected the decrease of R3 production than that of the input R2. In contrast, the simulations without back-hybridizations failed to explain the results of the experiments. In the simulations, R3 production monotonically increased with the initial concentrations of inputs R1 and R2, contradicting the results of the experiments. The fact that only the simulations with back-hybridizations explained the experiments suggests that the back-hybridizations are essential for describing the behavior of the AND gate reactions.

The effects of the back-hybridizations on the output R3 were further analyzed by simulating the time courses of the intermediates P3, P6, and Q3. P3 and P6 are closely involved in back-hybridizations BH1 and BH2, in Fig. 5, respectively. We did not focus on back-hybridization BH3 in Fig. 5 because BH3 has no substantial influence on output R3. In addition, the time course of Q3 was analyzed because Q3 transcribes R3, and thus, the production of Q3 determines the production of R3.

Figure 7 shows the time courses of P3, P6, Q3, and R3. Figures 7(a)–7(c) represent the time courses when $u_{R1}(0)=1$ and $u_{R2}(0)=0.5$, 2, and 8, respectively. At a higher $u_{R2}(0)$

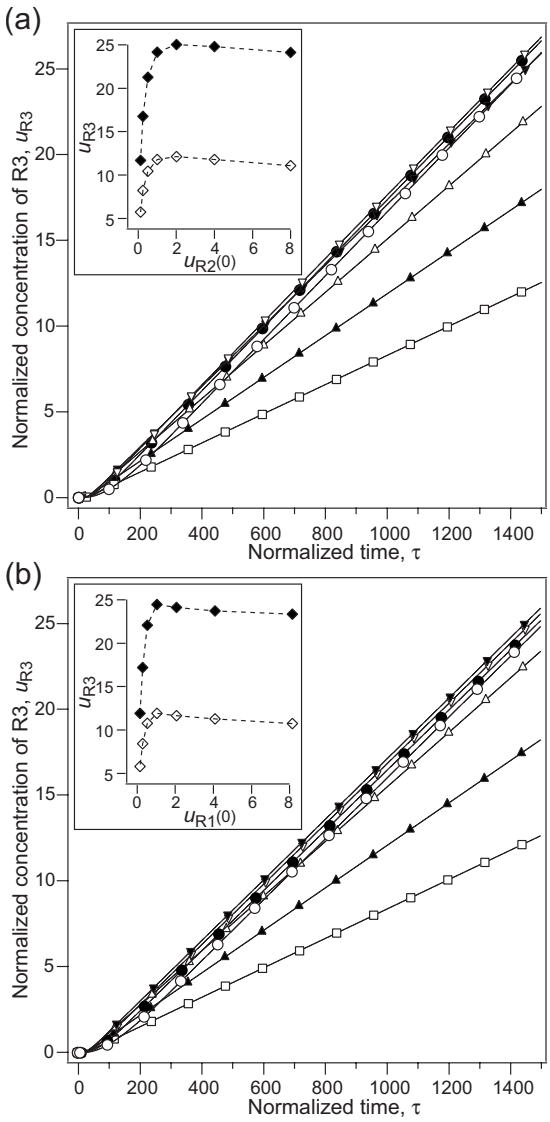

FIG. 6. Output production kinetics of AND gate in numerical simulations. (a) $u_{R2}(0)$ was changed from 0.125 to 8 with $u_{R1}(0)$ remaining at 1; $u_{R2}(0)=8$ (open circle), 4 (filled circle), 2 (open inverted triangle), 1 (filled inverted triangle), 0.5 (open triangle), 0.25 (filled triangle), and 0.125 (open square). Inset: dependence of R3 production on $u_{R2}(0)$ at $\tau=700$ (open diamond) and 1400 (filled diamond). (b) $u_{R1}(0)$ was changed from 0.125 to 8 with $u_{R2}(0)$ remaining at 1; $u_{R1}(0)=8$ (open circle), 4 (filled circle), 2 (open inverted triangle), 1 (filled inverted triangle), 0.5 (open triangle), 0.25 (filled triangle), and 0.125 (open square). Inset: dependence of R3 production on $u_{R1}(0)$ at $\tau=700$ (open diamond) and 1400 (filled diamond). $u_{R1}(0)$ and $u_{R2}(0)$ are normalized initial concentrations of R1 and R2, respectively.

[Fig. 7(c)], a large amount of P6 was produced, and the initial increase of Q3 was slower than that at a lower $u_{R2}(0)$ [Figs. 7(a)–7(c)], resulting in a slower initial increase of R3. Therefore, the slower initial increase of R3 was caused by the back-hybridization BH2. Figures 7(d)–7(f) represent the time courses when $u_{R2}(0)=1$ and $u_{R1}(0)=0.5$, 1, and 8, respectively. At a higher $u_{R1}(0)$ [Fig. 7(f)], a large amount of P3 was produced and the initial increase of Q3 was slower than that at a lower $u_{R1}(0)$ [Figs. 7(d) and 7(e)], resulting in

a slower initial increase of R3. Therefore, the slower initial increase of R3 was caused by the back-hybridization BH1. The back-hybridizations BH1 and BH2, which caused a slower initial increase of R3 with higher initial concentrations of R1 and R2, were thus found to prevent the R3 production from increasing monotonically with the initial concentration of the input RNA.

As shown in Fig. 6, R1 more strongly affected the decrease of R3 production than R2 did. This is also due to the back-hybridizations. From a comparison between Figs. 7(c) and 7(f), the saturated value of u_{Q3} at a high $u_{R1}(0)$ [Fig. 7(f)] was lower than that at a high $u_{R2}(0)$ [Fig. 7(c)]. In the case of the high $u_{R1}(0)$, back-hybridization BH1 slowed down the initial increase of Q3. In addition, back-hybridization BH2 reduced the saturated value of Q3 by wasting the input R2. In contrast, in the case of the high $u_{R2}(0)$, the back-hybridization BH2 only slowed down the initial increase of Q3. Therefore, as shown in Fig. 6, a high $u_{R1}(0)$ reduced the R3 production more than a high $u_{R2}(0)$ did.

V. DISCUSSION

We experimentally demonstrated that the AND gate of autonomous DNA computer RTRACS was successful under isothermal conditions. It produced the output RNA molecule R3 through a series of hybridization and enzymatic reactions only when both the input RNA molecules R1 and R2 were present. Although a set of reactions that implements the AND gate of RTRACS was proposed in our previous work [9], no experimental results of the AND gate have yet been reported. This study is the first report on experimental results that prove the successful implementation of the AND gate of RTRACS.

We also demonstrated that a mathematical modeling method for the AND gate of RTRACS successfully explained the experimentally observed behaviors of the AND gate. A set of rate equations describing molecular reactions of the AND gate was derived from its reaction scheme by assuming the two-state model of hybridization reactions and the Michaelis-Menten model of enzymatic reactions. The dependences of time courses of the output R3 on the initial concentrations of the inputs R1 and R2 were simulated by using the set of rate equations with the parameter values independently determined. The results of the kinetic simulations with consideration of back-hybridizations were consistent with the experimentally observed results: the output production of the AND gate increased at lower initial concentrations of inputs and slightly decreased at higher initial input concentrations. In the comparison, we focused only on the output R3 because the kinetic time courses of R3 can be experimentally measured more accurately than intermediates such as P3, P6, and Q3. These intermediates were more sensitive to the inputs as shown in Fig. 7. However, accurate measurements of their concentrations in the reaction mixtures of the AND gate are quite difficult because those intermediates cannot be specifically detected using molecular beacons or clearly separated on a gel.

Back-hybridizations, which affected the behavior of the AND gate of RTRACS, are commonly observed in many autonomous DNA computers. For example, the DNA molecular automaton by Shapiro *et al.* [1–3] and the Whiplash PCR machine by Hagiya *et al.* [4–6] also have back-hybridizations in their computing reactions. In the case of the DNA molecular automaton, the DNA strands that are cleaved and dissociated by the restriction enzyme *Fok*I reassociate with each other due to back-hybridizations, which results in the slowdown of the computing reactions. In the case of the Whiplash PCR machine, state transitions are inhibited by back-hybridizations as revealed by Rose *et al.* [6]. Therefore, back-hybridizations need to be considered in simulation models to develop autonomous DNA computers with high degrees of computational efficiency. The present mathematical modeling method succeeded in accounting for back-hybridizations, and thus improves the computational efficiency of RTRACS.

The modeling method for the AND gate of RTRACS demonstrated here will be crucial to construct novel and more complex computation elements, which can be derived from the molecular reactions of the AND gate. The simulations based on the modeling method offer overviews of the behaviors of computation elements even before time-consuming

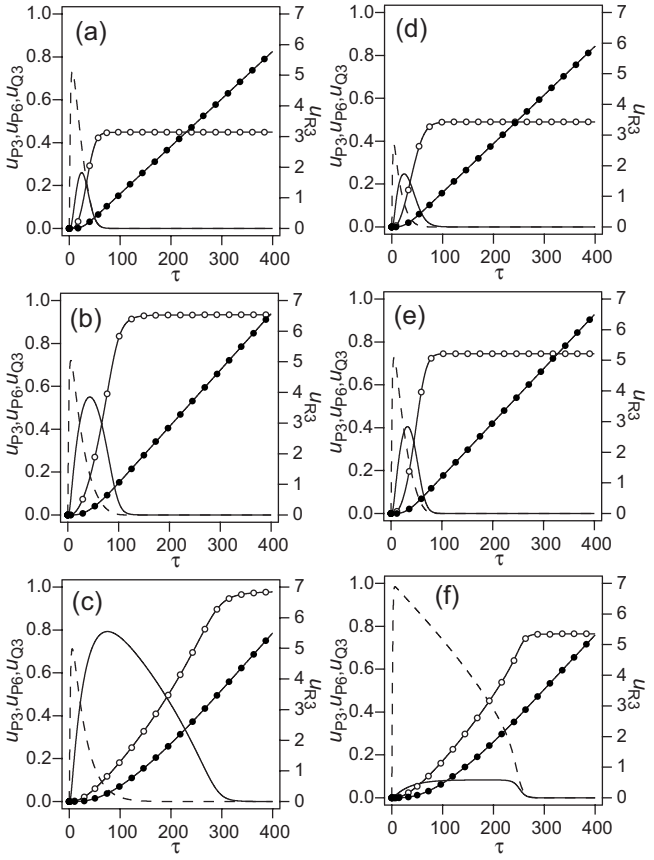

FIG. 7. Time courses of intermediates of AND gate in numerical simulations. P3 (broken line), P6 (solid line), Q3 (solid line with open circles), R3 (solid line with filled circles). (a) $u_{R1}(0)=1$, $u_{R2}(0)=0.5$. (b) $u_{R1}(0)=1$, $u_{R2}(0)=2$. (c) $u_{R1}(0)=1$, $u_{R2}(0)=8$. (d) $u_{R1}(0)=0.5$, $u_{R2}(0)=1$. (e) $u_{R1}(0)=1$, $u_{R2}(0)=1$. (f) $u_{R1}(0)=8$, $u_{R2}(0)=1$. $u_{R1}(0)$ and $u_{R2}(0)$ are normalized initial concentrations of R1 and R2, respectively.

experiments. We are now developing various logic gates and oscillatory reaction systems based on RTRACS working not only *in vitro* but also in small vesicles such as liposomes, and trying to apply them to genetic diagnosis of diseases and regulation of synthetic genetic circuits. Their development would be substantially facilitated by the mathematical modeling method reported here.

ACKNOWLEDGMENTS

We thank Dr. Mitsunori Takano and Dr. Hiroshi Yoshida for helpful discussions. We also thank Mr. Tetsuro Kitajima and Mr. YoungHun Lee for experimental support. This work was supported by a grant for SENTAN (Development of Systems and Technology for Advanced Measurement and Analysis) from the Japan Science and Technology Agency (JST), and by a grant-in-aid for the 21st Century COE program "Research Center for Integrated Science" and for Science Research on the Priority Area "Molecular Programming" from the Ministry of Education, Culture, Sports, Science, and Technology of Japan. M.T. acknowledges support from the Japan Society for the Promotion of Science.

APPENDIX: MICHAELIS-MENTEN MODEL IN COMPETITIVE ENZYMATIC REACTIONS

1. Basic Michaelis-Menten-type reaction without competition

The basic Michaelis-Menten-type reaction without competition of enzymes or substrates is represented as

$$\mathrm{E}_1 + \mathrm{I}_1 \underset{k_{-1}}{\overset{k_1}{\rightleftharpoons}} \mathrm{E}_1\mathrm{I}_1 \overset{k_1'}{\rightarrow} \mathrm{E}_1 + \mathrm{J}_1, \tag{A1}$$

where E_1 is the enzyme, I_1 is the substrate, and J_1 is the product. k_1, k_{-1}, and k_1' are rate constants. The rate equations are described as

$$\frac{d[\mathrm{J}_1]}{dt} = k_1'[\mathrm{E}_1\mathrm{I}_1], \tag{A2}$$

$$\frac{d[\mathrm{E}_1\mathrm{I}_1]}{dt} = k_1[\mathrm{E}_1][\mathrm{I}_1] - k_{-1}[\mathrm{E}_1\mathrm{I}_1] - k_1'[\mathrm{E}_1\mathrm{I}_1], \tag{A3}$$

$$[\mathrm{E}_1] + [\mathrm{E}_1\mathrm{I}_1] = [\mathrm{E}_1]_\mathrm{T}, \tag{A4}$$

where $[\mathrm{E}_1]_\mathrm{T}$ is the total concentration of E_1. Equation (A4) indicates the conservation law for E_1. In the Michaelis-Menten model, it is assumed that $[\mathrm{E}_1\mathrm{I}_1]$ immediately reaches its steady state; that is, $d[\mathrm{E}_1\mathrm{I}_1]/dt \approx 0$ in Eq. (A3) as follows:

$$0 = k_1[\mathrm{E}_1][\mathrm{I}_1] - k_{-1}[\mathrm{E}_1\mathrm{I}_1] - k_1'[\mathrm{E}_1\mathrm{I}_1]. \tag{A5}$$

Equations. (A4) and (A5) give

$$[\mathrm{E}_1\mathrm{I}_1] = \frac{[\mathrm{E}_1]_\mathrm{T}[\mathrm{I}_1]}{K_{\mathrm{m}1} + [\mathrm{I}_1]} \quad \left(K_{\mathrm{m}1} \equiv \frac{k_{-1} + k_1'}{k_1}\right). \tag{A6}$$

Therefore, from Eqs. (A2) and (A6), the rate equation for the product J_1 is obtained as

$$\frac{d[\mathrm{J}_1]}{dt} = \frac{k_{\mathrm{cat}1}[\mathrm{E}_1]_\mathrm{T}[\mathrm{I}_1]}{K_{\mathrm{m}1} + [\mathrm{I}_1]} = \frac{k_{\mathrm{cat}1}[\mathrm{E}_1]_\mathrm{T}[\mathrm{I}_1]}{K_{\mathrm{m}1}}\left[1 + \frac{[\mathrm{I}_1]}{K_{\mathrm{m}1}}\right]^{-1}, \tag{A7}$$

where $k_{\mathrm{cat}1} \equiv k_1'$.

2. Competition of multiple substrates for an enzyme

In the case that an enzyme competitively acts on two substrates, enzymatic reactions are represented as

$$\mathrm{E}_1 + \mathrm{I}_1 \underset{k_{-1}}{\overset{k_1}{\rightleftharpoons}} \mathrm{E}_1\mathrm{I}_1 \overset{k_1'}{\rightarrow} \mathrm{E}_1 + \mathrm{J}_1,$$

$$\mathrm{E}_1 + \mathrm{I}_2 \underset{k_{-2}}{\overset{k_2}{\rightleftharpoons}} \mathrm{E}_1\mathrm{I}_2 \overset{k_2'}{\rightarrow} \mathrm{E}_1 + \mathrm{J}_2, \tag{A8}$$

where E_1 is the enzyme, I_1 and I_2 are the substrates, and J_1 and J_2 are products from the respective substrates. k_1, k_{-1}, k_1', k_2, k_{-2}, and k_2' are rate constants. The rate equations are described as

$$\frac{d[\mathrm{J}_1]}{dt} = k_1'[\mathrm{E}_1\mathrm{I}_1], \tag{A9}$$

$$\frac{d[\mathrm{J}_2]}{dt} = k_2'[\mathrm{E}_1\mathrm{I}_2], \tag{A10}$$

$$\frac{d[\mathrm{E}_1\mathrm{I}_1]}{dt} = k_1[\mathrm{E}_1][\mathrm{I}_1] - k_{-1}[\mathrm{E}_1\mathrm{I}_1] - k_1'[\mathrm{E}_1\mathrm{I}_1], \tag{A11}$$

$$\frac{d[\mathrm{E}_1\mathrm{I}_2]}{dt} = k_2[\mathrm{E}_1][\mathrm{I}_2] - k_{-2}[\mathrm{E}_1\mathrm{I}_2] - k_2'[\mathrm{E}_1\mathrm{I}_2], \tag{A12}$$

$$[\mathrm{E}_1] + [\mathrm{E}_1\mathrm{I}_1] + [\mathrm{E}_1\mathrm{I}_2] = [\mathrm{E}_1]_\mathrm{T}, \tag{A13}$$

where $[\mathrm{E}_1]_\mathrm{T}$ is the total concentration of E_1 and Eq. (A13) expresses the conservation law for E_1. The steady states of $[\mathrm{E}_1\mathrm{I}_1]$ and $[\mathrm{E}_1\mathrm{I}_2]$, that is, $d[\mathrm{E}_1\mathrm{I}_1]/dt \approx d[\mathrm{E}_1\mathrm{I}_2]/dt \approx 0$, are assumed exactly as in the basic Michaelis-Menten model as follows:

$$\begin{aligned} 0 &= k_1[\mathrm{E}_1][\mathrm{I}_1] - k_{-1}[\mathrm{E}_1\mathrm{I}_1] - k_1'[\mathrm{E}_1\mathrm{I}_1] \\ &= k_2[\mathrm{E}_1][\mathrm{I}_2] - k_{-2}[\mathrm{E}_1\mathrm{I}_2] - k_2'[\mathrm{E}_1\mathrm{I}_2]. \end{aligned} \tag{A14}$$

Equations (A13) and (A14) give

$$[\mathrm{E}_1\mathrm{I}_1] = \frac{[\mathrm{E}_1]_\mathrm{T}[\mathrm{I}_1]}{K_{\mathrm{m}1}}\left[1 + \frac{[\mathrm{I}_1]}{K_{\mathrm{m}1}} + \frac{[\mathrm{I}_2]}{K_{\mathrm{m}2}}\right]^{-1}, \tag{A15}$$

$$[\mathrm{E}_1\mathrm{I}_2] = \frac{[\mathrm{E}_1]_\mathrm{T}[\mathrm{I}_2]}{K_{\mathrm{m}2}}\left[1 + \frac{[\mathrm{I}_1]}{K_{\mathrm{m}1}} + \frac{[\mathrm{I}_2]}{K_{\mathrm{m}2}}\right]^{-1} \tag{A16}$$

$$\left(K_{\mathrm{m}1} \equiv \frac{k_{-1} + k_1'}{k_1}, \quad K_{\mathrm{m}2} \equiv \frac{k_{-2} + k_2'}{k_2}\right). \tag{A17}$$

Therefore, the rate equation for the product J_1 is obtained from Eqs. (A9) and (A15) as follows:

$$\frac{d[\mathrm{J}_1]}{dt} = \frac{k_{\mathrm{cat1}}[\mathrm{E}_1]_{\mathrm{T}}[\mathrm{I}_1]}{K_{\mathrm{m1}}}\left[1 + \frac{[\mathrm{I}_1]}{K_{\mathrm{m1}}} + \frac{[\mathrm{I}_2]}{K_{\mathrm{m2}}}\right]^{-1}, \quad \text{(A18)}$$

where $k_{\mathrm{cat1}} \equiv k_1'$. The $[\mathrm{I}_2]/K_{\mathrm{m2}}$ is a contribution term from competition of I_2 for the enzyme, which is added to the equation for the noncompetitive rate equation (A7). Likewise, the rate equation for the product J_2 is obtained from Eqs. (A10) and (A16) as follows:

$$\frac{d[\mathrm{J}_2]}{dt} = \frac{k_{\mathrm{cat2}}[\mathrm{E}_1]_{\mathrm{T}}[\mathrm{I}_2]}{K_{\mathrm{m2}}}\left[1 + \frac{[\mathrm{I}_2]}{K_{\mathrm{m2}}} + \frac{[\mathrm{I}_1]}{K_{\mathrm{m1}}}\right]^{-1}, \quad \text{(A19)}$$

where $k_{\mathrm{cat2}} \equiv k_2'$. The term $[\mathrm{I}_1]/K_{\mathrm{m1}}$ represents the contribution from competition of I_1 for the enzyme.

In the case that an enzyme competitively acts on N substrates, rate equations for products are obtained in similar way to the above case of two substrates.

$$\frac{d[\mathrm{J}_i]}{dt} = \frac{k_{\mathrm{cat}i}[\mathrm{E}_1]_{\mathrm{T}}[\mathrm{I}_i]}{K_{\mathrm{m}i}}\left[1 + \frac{[\mathrm{I}_i]}{K_{\mathrm{m}i}} + \sum_{l\neq i}\frac{[\mathrm{I}_l]}{K_{\mathrm{m}l}}\right]^{-1} \quad (i = 1,2,\ldots,N), \quad \text{(A20)}$$

where I_i $(i=1,2,\ldots,N)$ is the substrate, and J_i is the product from I_i. The parameters $k_{\mathrm{cat}i}$ and $K_{\mathrm{m}i}$ are Michaelis-Menten parameters for I_i. The term $\Sigma_{l\neq i}[\mathrm{I}_l]/K_{\mathrm{m}l}$ represents the contribution from competition of all substrates except I_1. By using Eq. (A20), rate equations including competition of multiple substrates for an enzyme can be obtained.

3. Competition of multiple enzymes for a substrate

In the case that two enzymes competitively act on a substrate, enzymatic reactions are represented as

$$\mathrm{E}_1 + \mathrm{I}_1 \underset{k_{-1}}{\overset{k_1}{\rightleftharpoons}} \mathrm{E}_1\mathrm{I}_1 \overset{k_1'}{\rightarrow} \mathrm{E}_1 + \mathrm{J}_1,$$

$$\mathrm{E}_2 + \mathrm{I}_1 \underset{k_{-2}}{\overset{k_2}{\rightleftharpoons}} \mathrm{E}_2\mathrm{I}_1 \overset{k_2'}{\rightarrow} \mathrm{E}_2 + \mathrm{J}_2, \quad \text{(A21)}$$

where E_1 and E_2 are enzymes, I_1 is the substrate, and J_1 and J_2 are products by the two enzymes. k_1, k_{-1}, k_1', k_2, k_{-2}, and k_2' are rate constants. The rate equations are described as

$$\frac{d[\mathrm{J}_1]}{dt} = k_1'[\mathrm{E}_1\mathrm{I}_1], \quad \text{(A22)}$$

$$\frac{d[\mathrm{J}_2]}{dt} = k_2'[\mathrm{E}_2\mathrm{I}_1], \quad \text{(A23)}$$

$$\frac{d[\mathrm{E}_1\mathrm{I}_1]}{dt} = k_1[\mathrm{E}_1][\mathrm{I}_1] - k_{-1}[\mathrm{E}_1\mathrm{I}_1] - k_1'[\mathrm{E}_1\mathrm{I}_1], \quad \text{(A24)}$$

$$\frac{d[\mathrm{E}_2\mathrm{I}_1]}{dt} = k_2[\mathrm{E}_2][\mathrm{I}_1] - k_{-2}[\mathrm{E}_2\mathrm{I}_1] - k_2'[\mathrm{E}_2\mathrm{I}_1], \quad \text{(A25)}$$

$$[\mathrm{E}_1] + [\mathrm{E}_1\mathrm{I}_1] = [\mathrm{E}_1]_{\mathrm{T}}, \quad \text{(A26)}$$

$$[\mathrm{E}_2] + [\mathrm{E}_2\mathrm{I}_1] = [\mathrm{E}_2]_{\mathrm{T}}, \quad \text{(A27)}$$

where $[\mathrm{E}_1]_{\mathrm{T}}$ and $[\mathrm{E}_2]_{\mathrm{T}}$ are the total concentrations of E_1 and E_2, respectively. Equations (A26) and (A27) express the conservation laws of the enzymes. The steady states of $[\mathrm{E}_1\mathrm{I}_1]$ and $[\mathrm{E}_2\mathrm{I}_1]$ are assumed also in this case; that is, $d[\mathrm{E}_1\mathrm{I}_1]/dt \approx d[\mathrm{E}_2\mathrm{I}_1]/dt \approx 0$, so that

$$0 = k_1[\mathrm{E}_1][\mathrm{I}_1] - k_{-1}[\mathrm{E}_1\mathrm{I}_1] - k_1'[\mathrm{E}_1\mathrm{I}_1],$$

$$= k_2[\mathrm{E}_2][\mathrm{I}_1] - k_{-2}[\mathrm{E}_2\mathrm{I}_1] - k_2'[\mathrm{E}_2\mathrm{I}_1]. \quad \text{(A28)}$$

Equations (A26)–(A28) give

$$[\mathrm{E}_1\mathrm{I}_1] = \frac{[\mathrm{E}_1]_{\mathrm{T}}[\mathrm{I}_1]}{K_{\mathrm{m1}} + [\mathrm{I}_1]}, \quad \text{(A29)}$$

$$[\mathrm{E}_2\mathrm{I}_1] = \frac{[\mathrm{E}_2]_{\mathrm{T}}[\mathrm{I}_1]}{K_{\mathrm{m2}} + [\mathrm{I}_1]} \quad \text{(A30)}$$

$$\left(K_{\mathrm{m1}} \equiv \frac{k_{-1} + k_1'}{k_1}, \quad K_{\mathrm{m2}} \equiv \frac{k_{-2} + k_2'}{k_2}\right). \quad \text{(A31)}$$

Therefore, the rate equations for J_1 and J_2 are obtained from Eqs. (A22), (A23), (A29), and (A30) as follows:

$$\frac{d[\mathrm{J}_1]}{dt} = \frac{k_{\mathrm{cat1}}[\mathrm{E}_1]_{\mathrm{T}}[\mathrm{I}_1]}{K_{\mathrm{m1}}}\left[1 + \frac{[\mathrm{I}_1]}{K_{\mathrm{m1}}}\right]^{-1}, \quad \text{(A32)}$$

$$\frac{d[\mathrm{J}_2]}{dt} = \frac{k_{\mathrm{cat2}}[\mathrm{E}_2]_{\mathrm{T}}[\mathrm{I}_1]}{K_{\mathrm{m2}}}\left[1 + \frac{[\mathrm{I}_1]}{K_{\mathrm{m2}}}\right]^{-1}, \quad \text{(A33)}$$

where $k_{\mathrm{cat1}} \equiv k_1'$ and $k_{\mathrm{cat2}} \equiv k_2'$. If the two enzymes create an identical product $(\mathrm{J}_2 = \mathrm{J}_1)$, the rate equation for J_1 is a simple sum of the productions by E_1 and E_2 as follows:

$$\frac{d[\mathrm{J}_1]}{dt} = \frac{k_{\mathrm{cat1}}[\mathrm{E}_1]_{\mathrm{T}}[\mathrm{I}_1]}{K_{\mathrm{m1}}}\left[1 + \frac{[\mathrm{I}_1]}{K_{\mathrm{m1}}}\right]^{-1} + \frac{k_{\mathrm{cat2}}[\mathrm{E}_2]_{\mathrm{T}}[\mathrm{I}_1]}{K_{\mathrm{m2}}}\left[1 + \frac{[\mathrm{I}_1]}{K_{\mathrm{m2}}}\right]^{-1}. \quad \text{(A34)}$$

In the case that N enzymes competitively act on a substrate and create the identical product, rate equations for the product are obtained in similar way to the above case of two enzymes.

$$\frac{d[\mathrm{J}_1]}{dt} = \sum_{l=1}^{N}\frac{k_{\mathrm{cat}l}[\mathrm{E}_l]_{\mathrm{T}}[\mathrm{I}_1]}{K_{\mathrm{m}l}}\left[1 + \frac{[\mathrm{I}_1]}{K_{\mathrm{m}l}}\right]^{-1}, \quad \text{(A35)}$$

where I_1 is the substrate, J_1 is the product from I_1, and E_l $(l=1,2,\ldots,N)$ are the enzymes. The parameters $k_{\mathrm{cat}l}$ and $K_{\mathrm{m}l}$ are Michaelis-Menten parameters for E_l. By using Eq. (A35), rate equations including competition of multiple substrates for an enzyme can be obtained as a simple sum of the contribution from all enzymes.

[1] Y. Benenson, T. Paz-Elizur, R. Adar, E. Keinan, Z. Livneh, and E. Shapiro, Nature (London) **414**, 430 (2001).
[2] Y. Benenson, R. Adar, T. Paz-Elizur, Z. Livneh, and E. Shapiro, Proc. Natl. Acad. Sci. U.S.A. **100**, 2191 (2003).
[3] Y. Benenson, B. Gil, U. Ben-Dor, R. Adar, and E. Shapiro, Nature (London) **429**, 423 (2004).
[4] K. Sakamoto, D. Kiga, K. Komiya, H. Gouzu, S. Yokoyama, S. Ikeda, H. Sugiyama, and M. Hagiya, BioSystems **52**, 81 (1999).
[5] K. Komiya, K. Sakamoto, A. Kameda, M. Yamamoto, A. Ohuchi, D. Kiga, S. Yokoyama, and M. Hagiya, BioSystems **83**, 18 (2006).
[6] J. A. Rose, R. J. Deaton, M. Hagiya, and A. Suyama, Phys. Rev. E **65**, 021910 (2002).
[7] G. Seelig, D. Soloveichik, D. Y. Zhang, and E. Winfree, Science **314**, 1585 (2006).
[8] D. Y. Zhang, A. J. Turberfield, B. Yurke, and E. Winfree, Science **318**, 1121 (2007).
[9] N. Nitta and A. Suyama, Lect. Notes Comput. Sci. **2943**, 203 (2004).
[10] H. Yoshida and A. Suyama, DIMACS Series in Discrete Mathematics and Theoretical Computer Science **54**, 9 (2000).
[11] N. Nishida, T. Tanabe, K. Hashido, K. Hirayasu, M. Takasu, A. Suyama, and K. Tokunaga, Anal. Biochem. **346**, 281 (2005).
[12] T. Kitajima, M. Takinoue, K. Shohda, and A. Suyama, Lect. Notes Comput. Sci. **4848**, 119 (2008).
[13] M. Majlessi, N. C. Nelson, and M. M. Becker, Nucleic Acids Res. **26**, 2224 (1998).
[14] A. Tsourkas, M. A. Behlke, and G. Bao, Nucleic Acids Res. **30**, 5168 (2002).
[15] V. V. Didenko, BioTechniques **31**, 1106 (2001).
[16] T. A. Brown, *Molecular Biology LABFAX, I: Recombinant DNA*, 2nd ed. (Academic Press, New York, 1998), pp. 123–232.
[17] J. G. Wetmur, Crit. Rev. Biochem. Mol. Biol. **26**, 227 (1991).
[18] M. S. Krug and S. L. Berger, Biochemistry **30**, 10614 (1991).
[19] H. Yu and M. F. Goodman, J. Biol. Chem. **267**, 10888 (1992).
[20] C. T. Martin and J. E. Coleman, Biochemistry **26**, 2690 (1987).
[21] N. Hirano, M. Haruki, M. Morikawa, and S. Kanaya, Biochemistry **39**, 13285 (2000).